International Journal of Advanced Scientific Research
www.allscientificjournal.com
ISSN: 2456-0421
Received: 08-08-2026, Accepted: 07-09-2026, Published: 22-09-2026
Volume 11, Issue 3, 2026, Page No. 86-91

Synthesis, characterization of metal oxide nanoparticles using leaves of Tribulus terrestris, and evaluation of their antimicrobial potential

Pinki Meena[1], Payal Lodha[2*]
[1] Research Scholar, Department of Botany, University of Rajasthan, Rajasthan, India
[2] Professor, Department of Botany, University of Rajasthan, Rajasthan, India
DOI: https://doi.org/10.66856/ijasr.2026.11.3.11077

Abstract
The present study focuses on the green synthesis of zinc oxide (ZnO) and iron oxide (FeO) nanoparticles using *Tribulus terrestris* leaf extract and the evaluation of their antibacterial potential against selected pathogenic bacteria. The biosynthesized nanoparticles were characterized using FTIR, FESEM, zeta potential, and XRD analyses. FTIR results confirmed the involvement of phytochemicals such as phenolics, flavonoids, and proteins in the reduction and stabilization of nanoparticles. FESEM analysis revealed irregular, agglomerated nanostructures with rough surface morphology, while zeta potential measurements indicated good colloidal stability due to negatively charged surfaces. XRD patterns confirmed the crystalline nature and phase purity of the nanoparticles, with ZnONPs exhibiting a hexagonal wurtzite structure. The antibacterial activity was assessed against *Escherichia coli*, *Staphylococcus aureus*, *Bacillus subtilis*, and *Pseudomonas aeruginosa* using different concentrations (25–100 µg/ml). The results demonstrated a concentration-dependent increase in antibacterial activity, with nanoparticles showing significantly higher efficacy compared to plant extract. Among the tested samples, ZnONPs and FeONPs exhibited notable inhibitory effects, attributed to their nanoscale size, enhanced surface reactivity, and ability to generate reactive oxygen species. The findings suggest that *Tribulus terrestris*-mediated nanoparticles hold promising potential as effective antimicrobial agents for biomedical and environmental applications.

Keywords: Leaves of *Tribulus terrestris*, synthesis of znonps and feonps, characterization, antibacterial potential, etc

Introduction

Nanotechnology has emerged as a rapidly advancing field with significant applications in medicine, environmental science, and material engineering. Among various nanomaterials, metal oxide nanoparticles such as zinc oxide (ZnO) and iron oxide (FeO) have gained considerable attention due to their unique physicochemical properties, including high surface area, enhanced reactivity, and antimicrobial potential (Sirelkhatim *et al.*, 2015; Khan *et al.*, 2020) [10, 14]. These nanoparticles have been extensively explored for applications in drug delivery, water treatment, catalysis, and antimicrobial formulations. Particularly, ZnO nanoparticles are known for their strong antibacterial activity and biocompatibility, while iron oxide nanoparticles exhibit magnetic properties that make them suitable for biomedical and environmental applications (Gupta & Gupta, 2005) [6].

Conventional methods for nanoparticle synthesis often involve toxic chemicals, high energy consumption, and environmental hazards. In contrast, green synthesis using plant extracts has emerged as an eco-friendly, cost-effective, and sustainable alternative. Plant-mediated synthesis utilizes bioactive compounds such as flavonoids, phenolics, alkaloids, and proteins that act as reducing and stabilizing agents during nanoparticle formation (Iravani, 2011; Ahmed *et al.*, 2016) [1, 8]. *Tribulus terrestris*, a medicinal plant rich in phytochemicals, has been widely reported for its pharmacological properties, including antimicrobial, antioxidant, and anti-inflammatory activities. The use of such plant extracts not only enhances the biocompatibility of nanoparticles but also improves their biological efficiency through surface functionalization.

The increasing prevalence of antibiotic-resistant microorganisms has created an urgent need for alternative antimicrobial agents. Metal oxide nanoparticles have shown promising antibacterial activity against both Gram-positive and Gram-negative bacteria through mechanisms such as reactive oxygen species (ROS) generation, disruption of cell membranes, and interference with cellular metabolism (Slavin *et al.*, 2017; Raghupathi *et al.*, 2011) [11, 15]. In this context, the present study aims to synthesize ZnO and FeO nanoparticles using *Tribulus terrestris* leaf extract, characterize their physicochemical properties, and evaluate their antibacterial efficacy against selected pathogenic bacteria. The study highlights the potential of green-synthesized nanoparticles as effective and sustainable antimicrobial agents.

Materials and Methods

Collection and processing of plant material

Leaves of *Tribulus terrestris* were collected from campus, University of Rajasthan, Jaipur, Rajasthan. The healthy parts were taken and washed with running tap water to remove dust and dirt and then with distilled water to remove ionic impurities. The plant materials were dried in shade and grinded to make coarse powder. Those were extracted in distilled water. The extraction was done on a sonicator. 1 gram of dried plant material was dipped into 10 ml of distilled water and extracted on a sonicator for 10 minutes at 40°C. The extracted material was filtered using Whatmann's filter paper no. 1, and the filtrate was used for further use.

Green synthesis of metal oxide nanoparticles

The extracts of leaves were used to synthesize zinc oxide nanoparticles (ZnONPs). For ZnONPs, zinc sulfate salt was used, while for FeONPs, $FeCl_3$ salt was used. Salts were taken as 0.1 molar solutions. To synthesize nanoparticles, 90 ml of salt solution was kept on a magnetic stirrer, and 10 ml of the extract was added drop by drop. The mixture was stirred at 1200 rpm for 2 hours. Nanoparticles were separated by centrifuge at 15000 rpm for 10 minutes. Those were washed 3 times with distilled water by centrifuging at 5000 rpm for 5 minutes in each cycle. The obtained nanoparticles were collected in a crucible and kept in a muffle furnace at 1000°C for 15 minutes for calcination.

Characterization of the synthesized nanoparticles

FTIR analysis was performed using an FTIR spectrometer (PerkinElmer 95163). The dried NPs were mixed with KBr and pressed into pellets. The spectra were recorded in the range of 400-4000 cm^{-1} to identify functional groups associated with the nanoparticles. The morphology of the synthesized NPs was examined using FESEM (Zeiss). A small amount of NPs was mounted on a carbon tape and coated with gold before imaging to observe particle size and shape. EDX analysis was conducted in conjunction with FESEM to determine the elemental composition of the synthesized NPs. The weight percentage of zinc and oxygen was obtained to confirm the successful synthesis of metal oxide nanoparticles. The crystalline nature of NPs was evaluated using XRD (Panalytical Xpert Pro) in the 2θ range of 20° to 80°. The diffraction patterns were compared with standard patterns (JCPDS Card No. 36-1451) to confirm the hexagonal wurtzite structure of NPs. The stability of the synthesized NPs was assessed using a zeta potential analyzer (Zeta sizer Nano ZSP; ZEN 5600). A dilute suspension of NPs in distilled water was prepared, and the zeta potential was measured to determine the stability in aqueous media.

Determination of antibacterial potential

The antibacterial activity of green synthesized NPs and plant extracts was performed by the well diffusion method. *Escherichia coli* (MTCC1652), *Staphylococcus aureus* (MTCC3160), *Pseudomonas aeruginosa* (MTCC 741), and *Bacillus subtilis* (MTCC441) bacterial cultures were sub-cultured in Nutrient Agar and incubated at 37°C for 24 hours. Then the cultures were swabbed onto petri plates containing nutrient agar using a sterilized cotton swab. Wells of 6 mm in diameter were punctured onto the agar plates, and 25-100 µg/ml of sample solution was loaded into wells. The plates were incubated, and the zone of inhibition of each well was measured. Streptomycin (30 µg/ml) was used as a control to compare the effectiveness of samples against the tested bacteria. The activity index was calculated of dividing the inhibition zone of test sample by inhibition zone by the antibiotic drug. The experiments were conducted in triplicates.

Activity Index was calculated from comparison of activity of samples with the standard antibiotic drug. The activity index was calculated by the following formula:

Activity Index (AI) = Inhibition zone of sample/Inhibition zone of standard

Results and Discussion

Characterization of the synthesized nanoparticles

Fourier-Transform Infrared Spectroscopy (FTIR)

The FTIR spectrum of ZnO nanoparticles synthesized using *Tribulus terrestris* leaf extract confirms the active participation of leaf-derived phytochemicals in the reduction, capping, and stabilization of ZnO nanoparticles. A broad and intense absorption band observed around ~3322 cm^{-1} is attributed to O–H stretching vibrations of hydroxyl groups, indicating the presence of phenolic compounds, flavonoids, and alcohols, which are abundant in leaf tissues and play a major role in nanoparticle synthesis (Sirelkhatim *et al.,* 2015; Ahmed *et al.,* 2016) [1, 14]. The bands appearing at ~2922 cm^{-1} and 2855 cm^{-1} correspond to asymmetric and symmetric C–H stretching vibrations of aliphatic $–CH_2$ and $–CH_3$ groups, suggesting the involvement of lipids, terpenoids, and other organic constituents (Iravani, 2011) [8].

Fourier transform infrared (FTIR) spectroscopy was carried out to identify the functional groups involved in the green synthesis and stabilization of nanoparticles using leaf extract. The FTIR spectrum exhibits a broad absorption band around ~3320 cm^{-1}, corresponding to O–H stretching vibrations of hydroxyl groups from phenolic compounds and alcohols present in the leaf extract. Peaks observed at ~2922 and 2850 cm^{-1} are attributed to C–H stretching vibrations of aliphatic groups. The absorption band around ~1635 cm^{-1} corresponds to C=O stretching vibrations or amide I bands, indicating the presence of proteins and polyphenolic compounds (Sharma *et al.*, 2019) [13]. Peaks at ~1380 and 1320 cm^{-1} are associated with C–N stretching of amines. The strong absorption band observed in the region below ~600 cm^{-1} is assigned to Fe–O stretching vibrations, confirming the formation of iron oxide nanoparticles (Cornell & Schwertmann, 2003) [4].

The characteristic absorption bands at lower wavenumbers, particularly at ~880 cm^{-1} and ~653 cm^{-1}, correspond to Zn–O stretching vibrations, confirming the successful formation of ZnO nanoparticles (Sirelkhatim *et al.,* 2015) [14]. FTIR results demonstrate that *Tribulus terrestris* leaf extract is rich in functional biomolecules capable of effectively reducing and stabilizing ZnO nanoparticles, making the synthesized ZnONPs suitable for various biological and environmental applications.

Field Emission Scanning Electron Microscopy (FESEM)

Field Emission Scanning Electron Microscopy (FESEM) was employed to examine the surface morphology, particle distribution, and microstructural characteristics of the ZnO and FeO nanoparticles synthesized using *Tribulus terrestris* leaf extract. The FESEM image recorded at a magnification of 100 kX reveals that the ZnONPs exhibit predominantly irregular, flake-like, and fragmented morphologies with highly rough and uneven surfaces. The nanoparticles are densely packed and form large agglomerated clusters, which is a common feature of green-synthesized metal oxide nanoparticles due to strong interparticle interactions and high surface energy (Iravani, 2011; Khan *et al.*, 2020) [8, 10].

The FESEM micrograph reveals that the nanoparticles exhibit an irregular, aggregated morphology with rough and uneven surfaces. The particles appear to be clustered into larger agglomerates, which is commonly observed for iron oxide nanoparticles due to their magnetic nature and high surface energy (Gupta & Gupta, 2005) [6]. The surface texture suggests the presence of organic residues from the leaf extract coating the nanoparticles, supporting effective stabilization by phytochemicals (Ahmed *et al.*, 2016) [1].

FESEM analysis confirms the successful synthesis of porous, nanostructured ZnO and FeO nanoparticles with irregular morphology using *Tribulus terrestris* leaf extract, highlighting their potential effectiveness in environmental remediation, antimicrobial applications, antioxidant activity, and photocatalytic processes.

Zeta potential

Zeta potential analysis was performed to determine the surface charge characteristics and colloidal stability of the ZnO nanoparticles synthesized using *Tribulus terrestris* leaf extract. The zeta potential distribution curve exhibits a single, sharp, and narrow peak positioned in the negative potential region, indicating a uniform surface charge distribution among the nanoparticles. The presence of a dominant negative zeta potential confirms that the surface of the ZnONPs is negatively charged, which is attributed to the adsorption of plant-derived phytochemicals containing hydroxyl, carboxyl, and phenolic functional groups during the green synthesis process (Honary & Zahir, 2013) [7].

The zeta potential distribution shows a sharp peak centered near neutral to slightly negative values, indicating a relatively uniform surface charge distribution. This suggests moderate colloidal stability of the nanoparticles in aqueous suspension (Bhattacharjee, 2016) [3]. The observed stability is attributed to the adsorption of negatively charged phytochemicals from the leaf extract onto the FeONP surface, providing steric stabilization and preventing rapid aggregation.

The narrow peak width observed in the zeta potential distribution suggests good homogeneity and limited charge variability across the nanoparticle population, which contributes to improved dispersion stability in aqueous media. The negative surface charge generates electrostatic repulsive forces between individual nanoparticles, thereby reducing particle–particle aggregation and enhancing colloidal stability (Honary & Zahir, 2013) [7].

Zeta potential results confirm that the metal oxide nanoparticles synthesized via the green route using *Tribulus terrestris* leaf extract exhibit adequate surface charge stability, uniformity, and functionalized surfaces, which are essential for their effective performance in adsorption, antibacterial, antioxidant, and photocatalytic applications.

X-ray diffraction (XRD)

X-ray diffraction (XRD) analysis was performed to investigate the crystalline structure, phase formation, and crystallinity of the ZnO nanoparticles synthesized using *Tribulus terrestris* leaf extract. The XRD pattern recorded in the 2θ range of 10–80° exhibits several distinct and well-resolved diffraction peaks, confirming the crystalline nature of the synthesized ZnONPs. The prominent diffraction peaks correspond to the characteristic planes of ZnO and are in good agreement with standard JCPDS data (JCPDS card no. 36-1451), confirming the formation of the hexagonal wurtzite ZnO structure.

The most intense peak indicates preferential crystal growth along a specific plane and confirms the formation of crystalline ZnO. The absence of additional peaks related to impurities indicates high phase purity of the ZnONPs synthesized via the green route (Sirelkhatim *et al.*, 2015) [14].

For FeONPs, the XRD pattern displays characteristic diffraction peaks corresponding to crystalline iron oxide. The presence of sharp and intense peaks confirms crystallinity, while peak broadening suggests nanoscale crystallite size (Cullity & Stock, 2001) [5]. These findings are consistent with previously reported green synthesized iron oxide nanoparticles (Gupta & Gupta, 2005) [6].

The broadening of diffraction peaks suggests reduced crystallite size and lattice strain due to phytochemical-mediated synthesis. The crystallite size estimated using the Debye–Scherrer equation confirms the nanoscale range of the particles (Cullity & Stock, 2001) [5].

XRD results confirm the successful synthesis of phase-pure, crystalline nanoparticles with nanostructured characteristics using *Tribulus terrestris* leaf extract.

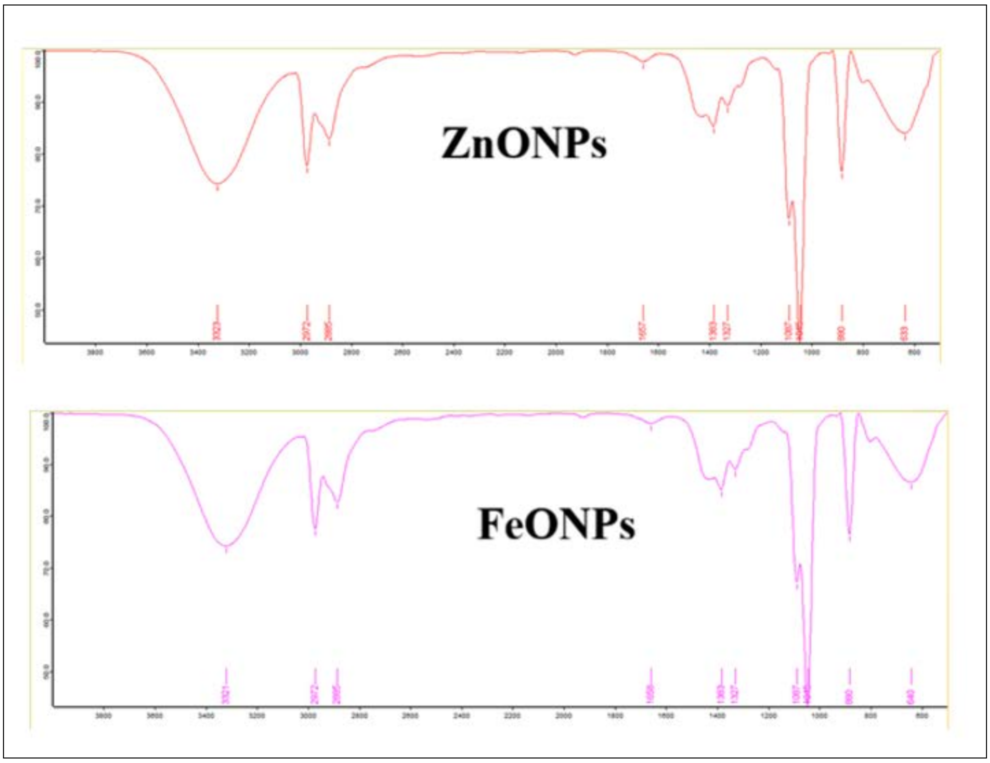

Fig 1: FTIR spectrum of nanoparticles using leaf extract of *T. terrestris*.

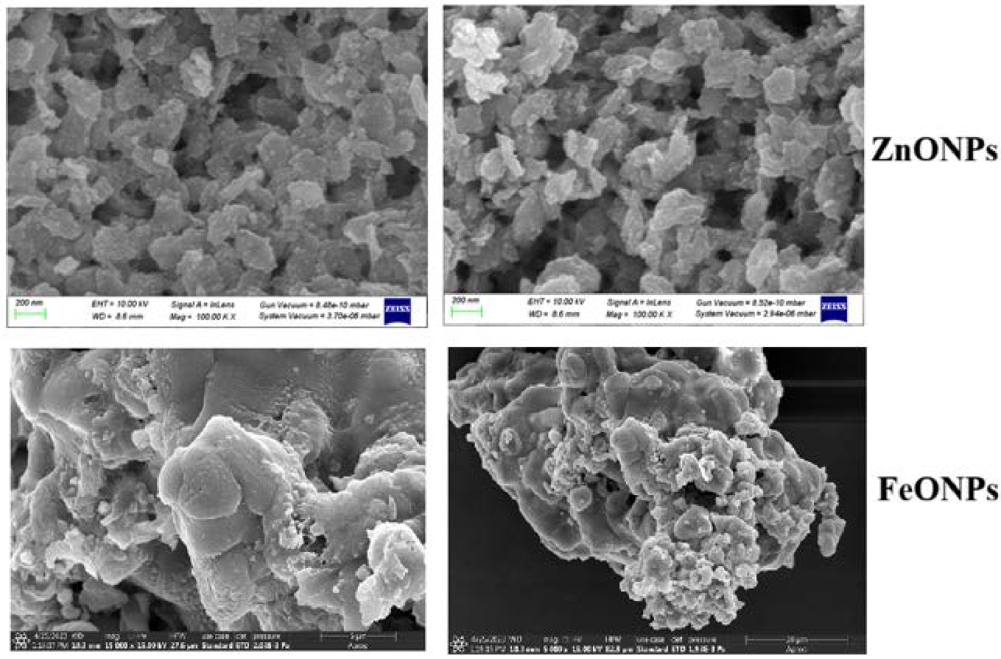

Fig 2: FESEM images of nanoparticles synthesized using leaf extract of *T. terrestris*.

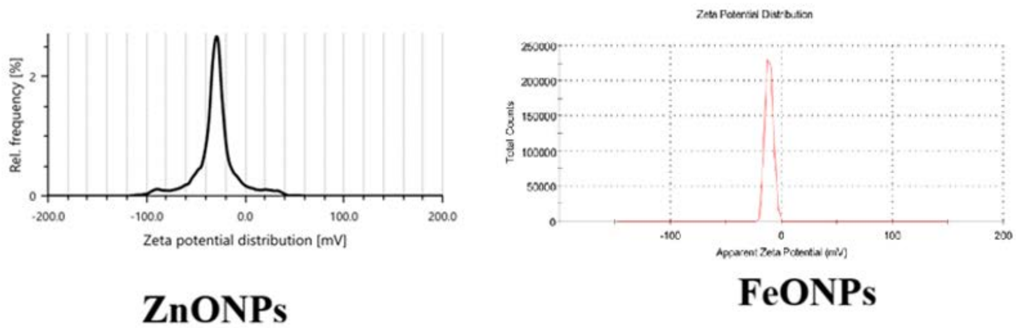

Fig 3: Zeta potential spectrum of nanoparticles synthesized using leaf extract of *T. terrestris*.

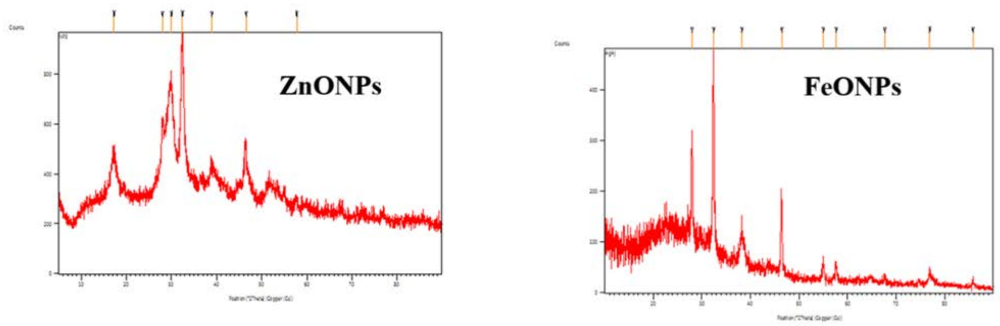

Peak List

Pos.[°2Th.]	Height [cts]	FWHMLeft[°2Th.]	d-spacing [Å]	Rel. Int. [%]
17.2417	172.34	0.8659	5.14316	29.38
28.0060	266.56	0.3464	3.18605	45.45
30.0052	383.92	0.8659	2.97816	65.46
32.4635	586.54	0.2598	2.75804	100.00
38.9277	89.77	0.6927	2.31365	15.31
46.5490	194.95	0.4330	1.95106	33.24
57.7734	34.26	0.6927	1.59588	5.84

Peak List

Pos.[°2Th.]	Height [cts]	FWHMLeft[°2Th.]	d-spacing [Å]	Rel. Int. [%]
28.0069	185.30	0.2362	3.18595	47.85
32.4338	387.28	0.2066	2.76050	100.00
38.2541	62.12	0.7085	2.35283	16.04
46.4641	127.56	0.3247	1.95443	32.94
55.0009	33.88	0.3542	1.66958	8.75
57.6529	31.80	0.3542	1.59893	8.21
67.6493	15.04	0.3542	1.38495	3.88
76.8834	24.98	0.3542	1.24001	6.45
85.8194	12.95	0.3542	1.13232	3.34

Fig 4: XRD spectrum of FeONPs synthesized using leaf extract of *T. terrestris*.

Evaluation of antibacterial potential

The antibacterial activity of *Tribulus terrestris* leaf extract, along with biosynthesized ZnO and FeO nanoparticles, was evaluated against both Gram-negative (*E. coli*, *P. aeruginosa*) and Gram-positive (*S. aureus*, *B. subtilis*) bacteria at different concentrations (25–100 µg/ml). The results clearly indicate a dose-dependent increase in antibacterial activity for all tested samples.

Among all treatments, FeONPs exhibited the highest antibacterial activity against *E. coli*, with the inhibition zone increasing from 9 mm at 25 µg/ml to 21 mm at 100 µg/ml (AI = 0.65). ZnONPs also showed significant activity (11–15 mm), whereas the crude plant extract demonstrated comparatively lower inhibition (10–13 mm).

This enhanced activity of nanoparticles may be attributed to their high surface area and reactive oxygen species (ROS) generation, which disrupt bacterial membranes (Raghupathi *et al.*, 2011) [11]. The superior performance of FeONPs at higher concentrations suggests stronger interaction with bacterial cell walls.

For *S. aureus*, ZnONPs showed slightly higher activity (11–15 mm) compared to FeONPs (10–16 mm), while plant extract remained least effective. The maximum activity index (0.42) was observed for FeONPs at 100 µg/ml.

Gram-positive bacteria are generally more susceptible to nanoparticles due to their thicker peptidoglycan layer, which facilitates nanoparticle adhesion and penetration (Baptista *et al.*, 2018) [2].

A similar trend was observed in *B. subtilis*, where ZnONPs demonstrated the highest inhibition (17 mm at 100 µg/ml), followed by FeONPs (14 mm) and plant extract (13 mm). The activity index increased proportionally with concentration, indicating effective bactericidal action of nanoparticles.

The results align with previous studies reporting that ZnO nanoparticles exhibit strong antimicrobial properties due to Zn^{2+} ion release and oxidative stress induction (Sirelkhatim *et al.*, 2015) [14].

P.aeruginosa showed relatively higher resistance compared to other bacteria; however, ZnONPs exhibited significant inhibition (10–18 mm; AI up to 0.66), followed by FeONPs and plant extract.

The relatively lower sensitivity of *P. aeruginosa* may be due to its intrinsic resistance mechanisms and outer membrane barrier, which limits nanoparticle penetration (Slavin *et al.*, 2017) [15].

Table 1: Antibacterial potential of plant extracts and the synthesized nanoparticles against various bacteria.

Name of bacteria	**Name of the sample**	**25 µg/ml**		**50 µg/ml**		**75 µg/ml**		**100 µg/ml**	
		IZ	AI	IZ	AI	IZ	AI	IZ	AI
E. coli	Leaves ZnONPs	11	0.45	12	0.4	14	0.45	15	0.46
	Leaves FeONPs	9	0.37	13	0.43	15	0.48	21	0.65
	Leaves P extract	10	0.41	11	0.36	12	0.38	13`	0.40
	Standard	24		30		31		32	
S. aureus	Leaves ZnONPs	11	0.35	13	0.37	14	0.38	15	0.39
	Leaves FeONPs	10	0.32	12	0.34	13	0.36	16	0.42
	Leaves P extract	9	0.29	10	0.28	11	0.30	13`	0.34
	Standard	31		35		36		38	
B. subtilis	Leaves ZnONPs	11	0.35	13	0.36	15	0.39	17	0.41
	Leaves FeONPs	9	0.29	11	0.30	12	0.31	14	0.34
	Leaves P extract	8	0.25	9	0.25	11	0.28	13`	0.31
	Standard	31		36		38		41	
P.aeruginosa	Leaves ZnONPs	10	0.45	13	0.56	16	0.59	18	0.66
	Leaves FeONPs	9	0.40	10	0.43	12	0.44	15	0.55
	Leaves P extract	8	0.36	9	0.39	11	0.40	13`	0.48
	Standard	22		23		27		27	

*IZ-Inhibition zone in mm; AI-Activity Index

Conclusion

The present study successfully demonstrates the green synthesis of zinc oxide (ZnO) and iron oxide (FeO) nanoparticles using *Tribulus terrestris* leaf extract as an eco-friendly and sustainable approach. Characterization studies (FTIR, FESEM, zeta potential, and XRD) confirmed the formation of stable, crystalline, and phytochemical-capped nanoparticles with desirable physicochemical properties. The antibacterial evaluation revealed a clear concentration-dependent activity, with ZnONPs and FeONPs exhibiting significantly higher efficacy than the crude plant extract against both Gram-positive and Gram-negative bacteria. The enhanced antimicrobial performance can be attributed to nanoscale size, increased surface reactivity, and reactive oxygen species generation. Findings highlight the potential of plant-mediated metal oxide nanoparticles as effective alternatives to conventional antimicrobial agents, with promising applications in biomedical, environmental, and pharmaceutical fields.

References

1. Ahmed S, Saifullah, Ahmad M, Swami BL, Ikram S. Green synthesis of silver nanoparticles using plant extracts. Journal of Advanced Research,2016:7(1):17–28.
2. Baptista PV, McCusker MP, Carvalho A, Ferreira DA, Mohan NM, Martins M, Fernandes AR. Nano-strategies to fight multidrug resistant bacteria—"A Battle of the Titans". Frontiers in Microbiology,2018:9:1441. https://doi.org/10.3389/fmicb.2018.01441.
3. Bhattacharjee S. DLS and zeta potential – What they are and what they are not? Journal of Controlled Release,2016:235:337–351.
4. Cornell RM, Schwertmann U. The Iron Oxides: Structure, Properties and Applications. Wiley-VCH, 2003.
5. Cullity BD, Stock SR. Elements of X-ray Diffraction. Prentice Hall, 2001.
6. Gupta AK, Gupta M. Synthesis and surface engineering of iron oxide nanoparticles. Biomaterials,2005:26(18):3995–4021.
7. Honary S, Zahir F. Effect of zeta potential on the properties of nano-drug delivery systems. Tropical Journal of Pharmaceutical Research,2013:12(2):255–264.

8. Iravani S. Green synthesis of metal nanoparticles using plants. Green Chemistry,2011:13:2638–2650.
9. Jones N, Ray B, Ranjit KT, Manna AC. Antibacterial activity of ZnO nanoparticle suspensions on a broad spectrum of microorganisms. FEMS Microbiology Letters,2008:279(1):71–76. https://doi.org/10.1111/j.1574-6968.2007.01012.x.
10. Khan I, Saeed K, Khan I. Nanoparticles: Properties, applications and toxicities. Arabian Journal of Chemistry,2020:13(12):9088–9106.
11. Raghupathi KR, Koodali RT, Manna AC. Size-dependent bacterial growth inhibition and mechanism of antibacterial activity of zinc oxide nanoparticles. Langmuir,2011:27(7):4020–4028. https://doi.org/10.1021/la104825u.
12. Rai M, Yadav A, Gade A. Silver nanoparticles as a new generation of antimicrobials. Biotechnology Advances,2009:27(1):76–83. https://doi.org/10.1016/j.biotechadv.2008.09.002.
13. Sharma G, Kumar A, Sharma S, Naushad M, Prakash Dwivedi R, Alothman ZA, Mola GT. Novel development of nanoparticles for green synthesis. Journal of King Saud University – Science,2019:31(2):257–269.
14. Sirelkhatim A, Mahmud S, Seeni A, Kaus NHM, Ann LC, Bakhori SKM, Hasan H, Mohamad D. Review on zinc oxide nanoparticles: Antibacterial activity and toxicity mechanism. Nano-Micro Letters,2015:7(3):219–242. https://doi.org/10.1007/s40820-015-0040-x.
15. Slavin YN, Asnis J, Häfeli UO, Bach H. Metal nanoparticles: Understanding the mechanisms behind antibacterial activity. Journal of Nanobiotechnology,2017:15:65. https://doi.org/10.1186/s12951-017-0308-z.